Non-Parametric Synchronization Measures used in EEG and MEG

Marco Congedo

▶ To cite this version:

Marco Congedo. Non-Parametric Synchronization Measures used in EEG and MEG. [Technical Report] GIPSA-lab. 2018. hal-01868538v2

HAL Id: hal-01868538
https://hal.science/hal-01868538v2

Submitted on 23 Sep 2019

Technical Report

Non-Parametric Synchronization Measures used in EEG and MEG

~

Marco Congedo

GIPSA-lab, CNRS, University Grenoble-Alpes, Grenoble INP.
Address : GIPSA-lab, 11 rue des Mathématiques, Grenoble Campus BP46, F-38402, France

Introduction

Any time-domain signal can be equivalently represented in the frequency domain. Such representation is appropriate to estimate the average of spectral measures over time. However, often it is of interest to study the temporal dynamics of EEG data, for example in ERP analysis, thus in EEG literature we see more and more studies using time-frequency analysis (TFA). TFA decomposes a time series in a two dimensional plane, with one dimension being the *time* and the other being the *frequency*. One can then perform the analysis for any number of frequencies along time. In this section we will explain and describe univariate and bivariate spectral measures in the frequency and time-frequency (TF) domain. In the discussion we will consider some of the technical concerns that should be addressed in practice. Throughout this article will denote by x an EEG segment recorded at one channel or at any other derivation, such as a source component, for example a source component derived by independent component analysis (Makeig et al., 2004) or, more in general, by blind source separation techniques (Congedo, Gouy-Pailler and Jutten, 2008). Notice that we will enclose in brackets $<>$ an empirical average over K realizations (i.e., $\langle a \rangle = \frac{1}{K}\sum_{k=1}^{K} a_k$), using the usual notation in the right-end side only when necessary to avoid confusions. This will allow us to simplify notation considerably and to make more apparent the different ways in which averages can be taken.

Frequency Domain Analysis

The fundamental mathematical tool for harmonic analysis is the Discrete Fourier Transform (DFT). The DFT decomposes a finite signal as a finite sum of sinusoids with different *frequency*, *amplitude* and *phase*. It can be computed efficiently by means of the celebrated Fast Fourier Transform (FFT) algorithm (Cooley and Tukey, 1965; Frigo and Johnson, 2005). The DFT of the signal in x results in a complex number $z_f = a_f + ib_f$ for each discrete Fourier frequency f [1]. a_f and b_f are real numbers and are named the FFT coefficients. The univariate measures of interest are the *amplitude* and *phase* at frequency f, given by the *modulus* of z_f, $r_f = |z_f| = \sqrt{a_f^2 + b_f^2}$ and by its *argument* $\varphi_f = Arg(z_f) = ArcTan(b_f/a_f)$, respectively. The amplitude and phase are real quantities and have a straightforward geometrical interpretation in the complex plane (Fig. 3);

---

[1] If x holds M samples and letting $m=M/2$, the DFT of x results in $m+1$ of such complex numbers, corresponding to frequencies 0 (direct current), $1/L$, $2/L$,…,m/L, where L is the frequency resolution, given by the reciprocal of the number of seconds in x. For example, if x holds two seconds of data, the frequency resolution L will be $1/2=0.5$Hz. M is typically chosen as a power of 2, a typical requirement of FFT algorithms.

in the DFT, for each frequency f, r_f is the amplitude of the decomposed sinusoid and φ_f is its position in time (lag). The set of values $r_f{}^2$ and φ_f along all discrete frequencies provides then the *power spectrum* and *phase spectrum*, respectively.

In order to analyze continuous EEG time-series of arbitrary duration, the standard methods is averaging the power spectrum across sliding overlapping windows (Welch, 1967). In ERP and ERD/ERS analysis the multiple realizations are sweeps time-locked to an event and we can conveniently average across sweeps. The phase spectrum is rarely analyzed, since the phase of the signal is more conveniently studied by means of TFA. Bivariate measures in the frequency domain such as coherence have identical expressions as in TFA, so without loss of generality we will treat them in the framework of TFA.
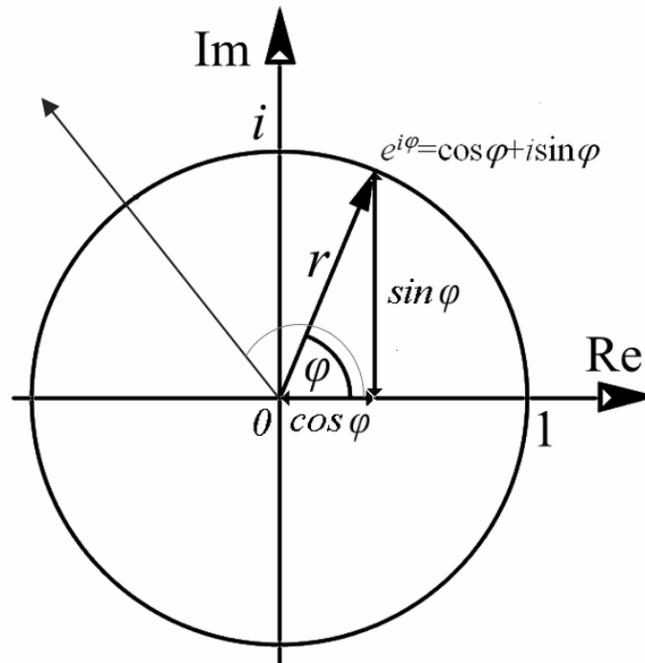

Figure 3: In the complex plane the abscissa is the real line and the ordinate is the imaginary line endowed with the imaginary unit i, which is defined as $i^2 = -1$. A complex number z can be represented in Cartesian coordinates as $\Re(z) + i\Im(z)$, where $\Re(z)$ is the real coordinate and $\Im(z)$ the imaginary coordinate. It can also be represented by a position vector, that is, the vector joining the origin and the point, with length r and angle φ, the angle being defined with respect to the real axis. r and φ are known as the polar coordinates of a complex number. More, in trigonometric form the coordinates are $r\cos\varphi$ and $ir\sin\varphi$, therefore, using Euler's formula $e^{i\varphi} = \cos\varphi + i\sin\varphi$, we can also express any complex number as $re^{i\varphi}$. This reduces to $e^{i\varphi}$ if the point is on the unit circle (i.e., wherever $r=1$), which is the case of the thick vector in the figure. In the frequency domain we obtain a complex number for each frequency. In the time-frequency domain we obtain a complex number for each time-frequency point. Regardless the representation, the amplitude r is expressed in μV units, while the phase φ, which is a circular quantity, is usually reported in the radians interval $(-\pi, \ldots, \pi]$ or $(0, \ldots, 2\pi]$.

Time-Frequency Domain Analysis

Whereas several possible time-frequency (TF) representations exist, in the EEG literature we mainly encounter two of them, namely, the *analytic signal* resulting from the *Hilbert transform* (Chavez et al. 2006; Rosenblum et al., 1996; Tass et al., 1998) and *wavelets* (Lachaux et al., 1999; Tallon-Baudry et al., 1996). Several studies comparing the Hilbert transform to wavelets have found that the two representations give very similar results (Burns, 2004; Le Van Quyen et al., 2001; Quian Quiroga et al., 2002).

The Analytic Signal

The analytic signal (Gabor, 1946) is efficiently computed by means of the FFT algorithm, as described concisely by Marple (1999). The *analytic signal* representation of time-series x has the form $z=x+iy$, where y is the *Hilbert transform* of x. z is a *complex signal in the time domain* with the same sampling rate as the original signal. By applying a filter bank to the signal, that is, a series of band-pass filters centered at successive frequencies f (for example, centered at 1Hz, 2Hz, …) and by computing the Hilbert transform for each filtered signal, we obtain the analytic signal in the TF domain, that is, for all points $z_{tf}=x_{tf}+iy_{tf}$ in the TF plane. In analogy to what we have done in the frequency domain, from z_{tf} we obtain the *analytic amplitude* r_{tf}, also known as the *envelope*, and the *analytic phase* φ_{tf}, as the modulus and argument of z_{tf}, respectively[2]. These quantities are the polar coordinates of the analytic signal (Fig. 3), which we may write as $z_{tf} = r_{tf}e^{i\varphi_{tf}}$. The physical interpretation of these quantities in is illustrated in Fig. 4.

---

[2] Often they are named *instantaneous amplitude* and *instantaneous phase*. Here we prefer keeping the denomination "analytic" since "instantaneous" is used in this chapter in opposition to "lagged" to indicate a particular kind of phase relationships.
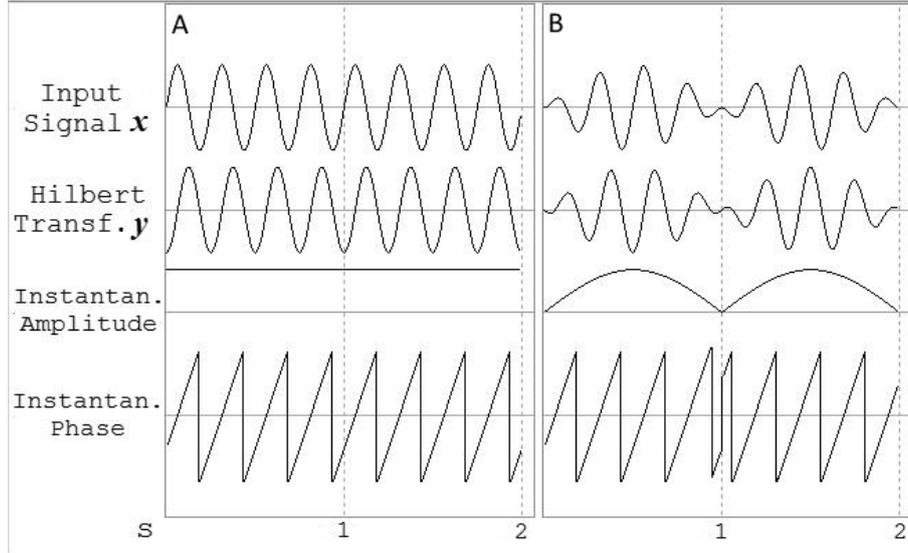
Figure 4: Two 2-second signals are shown as the top traces (*x*). Time is on the abscissa. The vertical scaling of the last traces is arbitrary. The analytic signal is *z=x+iy*, where *y* is the Hilbert transform of the input signal and is shown as the second trace. The next two traces are the analytic amplitude (envelope) and analytic phase. Note that the envelope is a non-negative quantity. A): the input signal is a sine wave at 4Hz. The instantaneous amplitude is constant in the whole epoch. The phase oscillates regularly in between its bounds at 4Hz. B): the input signal is a sine wave at 4Hz multiplied by a sine wave at 0.5 Hz with the same amplitude. The result input signal is a sine wave at 4Hz, which amplitude is modulated by the sine wave at 0.5Hz. The phase features an abrupt change at 1s, which may be misinterpreted as a phase resetting phenomenon.

Computing Ensemble Averages in the Time-Frequency Domain

In order to increase the signal-to-noise ratio, the analytic signal is usually averaged across short time segments and/or adjacent frequencies. In the following we will drop the time and frequency subscripts t and f whenever not necessary, assuming that the analytic signal z under analysis refers to a single TF point or that it has been averaged within neighboring TF points before computing the average across realizations. As a matter of fact, all measures we will consider makes use of two different ways to obtain averages and they determine to what physiological phenomena the measure is sensitive. Let $z_k=x_k+iy_k$ be the analytic signal evaluated at realization k. Suppose we average the envelope across realizations as $\langle |z| \rangle = \frac{1}{K} \sum_k \sqrt{x_k^2 + y_k^2}$. In this case the average envelope depends on the absolute magnitude of the x_k and y_k coefficient, ignoring completely their phase. Thus, $\langle |z| \rangle$ is sensitive to all kinds of activity, may it be phase-locked or not. We may also average the analytic signal directly as $\langle z \rangle = \frac{1}{K} \sum_k x_k + i \frac{1}{K} \sum_k y_k$, from which the average analytic amplitude and analytic phase are given by $|\langle z \rangle|$ and $\arg\langle z \rangle$, respectively. Note that $|\langle z \rangle|$ may be high only if the realizations

5

have a *preferred phase* at that time-frequency point, whereas if the phase is randomly distributed around the circle, $\left|\langle z\rangle\right|$ will tend toward zero. This phenomenon if illustrated in Fig 5. As a consequence, $\left|\langle z\rangle\right|$ is a measure of *Concentration* (inverse of *phase variance*) that is sensitive to phase-locked activity only (e.g., *evoked* ERP components), while $\arg\langle z\rangle$ measures the phase *preferred direction* (mean direction). These considerations should be kept in mind for interpreting the measures we will describe.
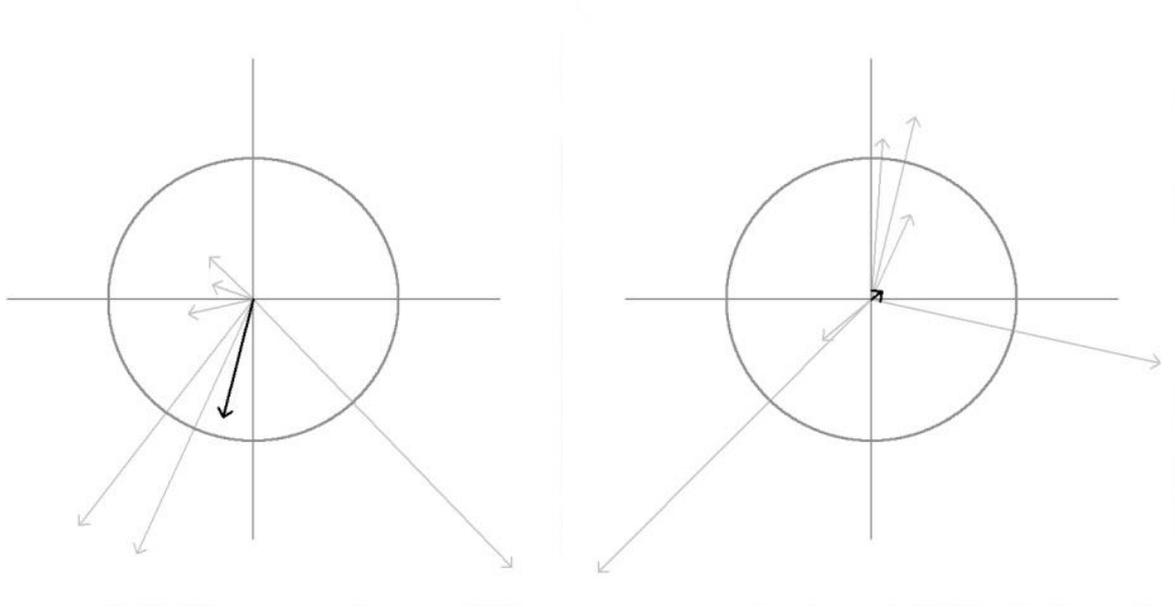

Figure 5: In each diagram six complex numbers are represented as position vectors (gray arrows) in the complex plane (see Fig. 3). Consider these vectors as representing the analytic signal for a given time-frequency point or time-frequency region estimated on six different ERP sweeps. In each diagram the black arrow is the position vector corresponding to the average of the six complex numbers, i.e., the average analytic signal across the six sweeps $\left|\langle z\rangle\right|$. In the left diagram the vectors are distributed within one half circle, featuring a preferred direction. In the right diagram the vectors are randomly distributed around the circle; the resulting mean vector is much smaller, although the average length of the six vectors $\left\langle|z|\right\rangle$ in the two diagram is approximately equal.

Linear and Non-Linear Measures of amplitude, phase concentration and phase mean

Based on these considerations, for analytic signal z at whatever TF region we define three fundamental linear univariate measures: the analytic signal *mean amplitude* (*MAmp*), the *concentration* (*Con*) and the *mean direction* (*MDir*) such as

$$MAmp = \left\langle|z|\right\rangle = \left\langle\left|re^{i\varphi}\right|\right\rangle = \left\langle\sqrt{x^2+y^2}\right\rangle , \tag{0.1}$$

$$Con = \left|\langle z \rangle\right| = \left|\langle re^{i\varphi} \rangle\right| = \sqrt{\langle x \rangle^2 + \langle y \rangle^2} \quad \text{and} \tag{0.2}$$

$$MDir = ArcTan \frac{\langle y \rangle}{\langle x \rangle} . \tag{0.3}$$

Note that it does not make sense to average directly phase values φ_k estimated at each realization, i.e., to define a measure such as $ArcTan\left(\langle y/x \rangle\right)$ [3].

These three measures are elementary quantities reported ubiquitously in the literature for a wide spectrum of purposes, in a great variety of variants and combinations. Often, new name are given to existing measures, or the same measure is named differently in different articles, increasing the confusion of the non-expert reader. Nonetheless, these three measures are the fundamental bricks of univariate measures. For example, in a frequency domain study on epilepsy, Kalitzin et al. (2002) define a "phase clustering" measure as *Con/MAmp* and look at how such measure changes when evaluated at the frequency of intermittent photic stimulation and its higher harmonics.

An important non-linear TF measures may be obtained adding a simple normalization of the analytic signal. Let again $z_k = x_k + iy_k$ be the analytic signal at realization k. Now, before computing the average across realizations, replace x_k by x_k/r_k and y_k by y_k/r_k , where $r_k = |z_k| = \sqrt{x_k^2 + y_k^2}$ .This means that at all TF points and at each realization the vector $x_k + iy_k$ is stretched or contracted so as to be constrained on the unit complex circle (Fig. 6). Although deceivingly simple, this normalization is highly non-linear (Pascual-Marqui, 2007). After normalization, the *MAmp* measure (0.1) becomes meaningless, as it is always equal to 1; the *Con* measure on the other hand will be now actually sensitive to the variance of the phase across realizations *regardless of amplitude,* that is, it will be a measure depending only on phase. In the literature on circular (directional) statistics, which traces back to the work of Lord Reyleigh and Karl Pearson (Mardia, 1972), this is known as the "circular mean resultant length". In the EEG literature it is known as inter-trial phase coherence (Makeig et al., 2002, 2004), but has been named by different authors also "inter-trial phase clustering" and "phase coherence" among other ways (Cohen, 2014, p. 243). In this chapter we will refer to it as to *phase concentration* (*PCon*), where here and hereafter the prefix "Phase" is added to its non-

---

[3]Like phase, the time of the day is also a circular quantity and provides a good example. An appropriate average of 22h and 1h is 23h30, but this is very far from their arithmetic mean. See also Cohen (2014, pp 214-246).

normalized counterpart to stress the strictly dependence on phase of the measure. After the normalization the *PCon* measure simplifies to (see (0.2), Fig. 3 and Fig. 6)

$$PCon = \left| \left\langle e^{i\varphi} \right\rangle \right| ,$$

(0.4)

and the corresponding *phase mean direction (PMDir)* is

$$PMDir = ArcTan = \frac{\left\langle y/r \right\rangle}{\left\langle x/r \right\rangle}$$

(0.5)

Note that *PCon* is bounded between 0 (random phase distribution across realizations) and 1 (all vectors point in the same direction). This will be the case for all measures described hereafter. We say in this case that the measure is *dimensionless*.
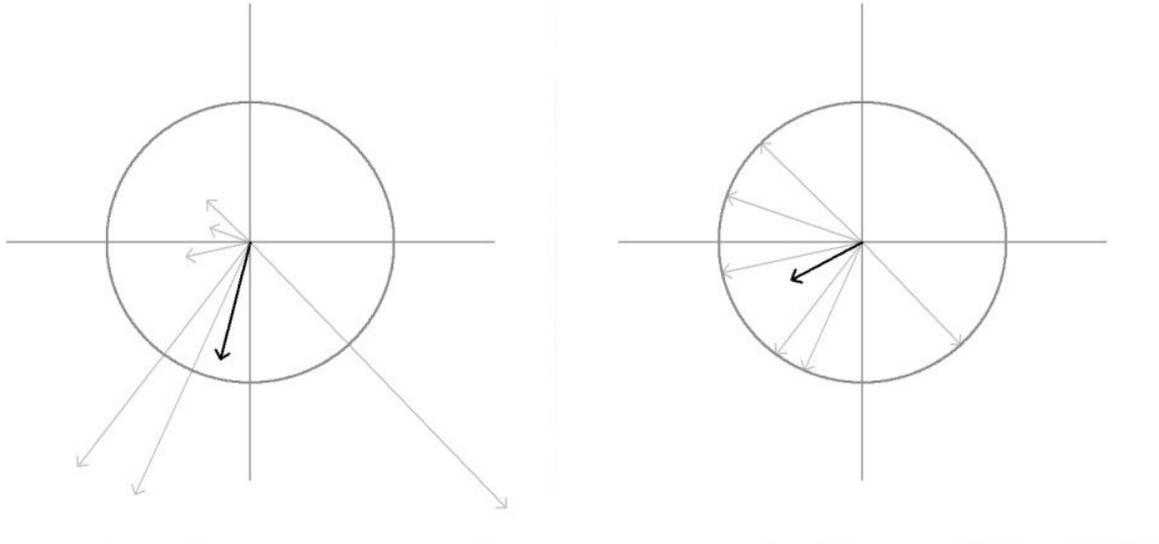

Figure 6: The left diagram is the same as in Fig. 5. The vectors in the right diagram have been normalized to unit length (non-linear normalization), that is, we replace $re^{i\varphi}$ by $e^{i\varphi}$. Note that the mean vector in the right points in a different direction as compared to the mean vector on the left, albeit the vectors have the same direction in the two diagrams; the average is weighted by the amplitude of the vectors in the left plot, whereas it ignores the amplitude in the right plot.

A number of interesting measures can be obtained by computing a *weighted average* of the normalized analytic signal $e^{i\varphi}$. Thinking this way, *Con* (0.2) is the non-normalized average analytic signal $\left| \left\langle re^{i\varphi} \right\rangle \right|$, that is, it is equal to the *PCon* weighted by its own envelope. Choosing the weights differently we obtain quiet different measures of phase concentration.

Weights can be given by experimental or behavioral variables such as reaction time, stimulus luminance, etc. In this way, we can discover phase concentration effects that are specific to certain properties of the stimulus or certain behavioral responses (Cohen and Cavanagh, 2011). We will refer to this measure as to the *weighted phase concentration* (*wPCon*). If w_k are the weights (assumed non-negative), it is given by

$$wPCon = \frac{\left|\left\langle we^{i\varphi}\right\rangle\right|}{\left\langle w\right\rangle}$$ (0.6)

Next, consider two distinct frequencies, which we name here the *amplitude frequency* f_a and the *phase frequency* f_p. Typically, $f_p < f_a$. Weighting the normalized analytic signal at the phase frequency by the envelope of the signal at the amplitude frequency we obtain a popular measure of cross-frequency coupling named *modulation index* (*MI*: Canolty et al., 2006; Cohen, 2014, p. 413). The normalized version of this measure is the *phase-amplitude coupling* (*PAC*), which is the *MI* normalized by the amplitude (Özkurt and Schnitzler, 2011). This is given by

$$PAC = \frac{\left|\left\langle r_{f_a} e^{i\varphi_{f_p}}\right\rangle\right|}{\left\langle r_{f_a}\right\rangle}$$ (0.7)

If the phase distribution at the phase frequency is uniform, high values of *PAC* indicates that the phase frequency modulates the signal at the amplitude frequency. Özkurt and Schnitzler (2011) proposed to use $\sqrt{\left\langle r_{f_a}^2\right\rangle}$ instead of $\left\langle r_{f_a}^2\right\rangle$ as normalization in (0.7). Such an expression can be used also in the denominator of other normalized measures we encounter in this section, however using such normalization the obtained measure is sensitive to the variance of the normalizing random variables, here r_{f_a}: the higher the variance of the amplitude r_{f_a} the lower the resulting PAC. We therefore present all measures with a normalization of the form as in (0.7), keeping in mind that other form of normalizations may suits better the experimental purposes.

Both the *wPCon* and the *MI* measures are subjected to several confounding effects. As a consequence, they cannot be interpreted as they are, instead they must be standardized, for example, using resampling methods (for details see Canolty et al., 2006 and Cohen, 2014, p.

253-257 and p. 413-418). The standardized *MI* and *PAC*, along with their bivariate extensions discussed in next sub-section, are used to study an important class of phenomena that can be found in the literature under the name of phase-amplitude nesting (or coupling, interaction, binding), amplitude modulation and more (Colgin, 2015; Lisman and Jensen, 2013; Llinas, 1988; Freeman, 2015; Palva and Palva, 2012; Varela et al., 2001). Nonetheless, the *MI* and *PAC* measure do not allow a straightforward physical interpretation and may issue unexpected results when applied to simulated data, therefore they should be used with caution.

Bivariate Measures in the Frequency and Time-Frequency Domain

A large family of bivariate measures are measures of dependency in the TF domain evaluating de facto the degree of *amplitude co-modulation* and/or *phase synchronization* between two time series over time. Two such measures are very popular in the EEG literature. They are known as the *coherence* (Nunez et al., 1997; Shaw, 1981) and *phase coherence*, the latter being known also as the *phase-locking value* (Lachaux et al., 1999; Mormann et al., 2000; Rosenblum et al., 1996; Tass et al., 1998). For any analytic signal $z=x+iy$ in whatever TF point or region, the *auto-spectrum*

$$c = zz^* = x^2 + y^2 = r^2 \tag{0.8}$$

(superscript * indicates complex conjugate[4]) is a real quantity providing the squared amplitude (*power)* of the signal, that is, the TF-domain equivalent of the signal *variance*, which is a natural measure of the signal *energy*. Given two analytic signals z_1 and z_2 in whatever TF regions, the *cross-spectrum* between them is the TF domain equivalent of their *covariance* and is given by

$$c_{12} = z_1 z_2^* = r_1 r_2 e^{i(\varphi_1 - \varphi_2)}. \tag{0.9}$$

The *coherence* measure is defined as

$$Coh = \frac{\left| \langle c_{12} \rangle \right|}{\sqrt{\langle c_1 \rangle \langle c_2 \rangle}}, \tag{0.10}$$

which is the equivalent of Pearson's correlation in the TF-domain, taken in its absolute value. This is the bivariate extension of the *Con* (0.2) measure (with, as usual, the normalization in the denominator bounding the measure in between 0 and 1). The right-end side expression in (0.9)

---

[4] The complex conjugate of a complex number $a+ib$ is $a-ib$.

shows that the cross-spectrum is a function of both the *relative phase* ($\varphi_1 - \varphi_2$) of the two signals and the product of their amplitude $r_1 r_2$. Hence, when averaging cross-spectra, coherence will be influenced both by the *phase synchronization* (dependency of angles $\varphi_1 - \varphi_2$ over realizations) and by the *amplitude co-modulation* (dependency of amplitudes $r_1 r_2$ over realizations). Phase synchronization depends on the *concentration of the relative phase*. If the distribution of the relative phase is uniformly distributed across realizations the coherence will be zero. Amplitude co-modulation instead depends on the *covariance of the two amplitudes*. If the two amplitudes are uncorrelated across realizations, the coherence will be zero. Thus, coherence increases both with phase synchronization and amplitude co-modulation across realizations. This has been often been pointed out as a limitation of coherence, since it is difficult to disentangle the two effects (Lachaux et al., 1999). In order to do so we can decompose the terms in the right-end side of (0.9). First, we define a measure of amplitude *co-modulation*, such as

$$Com = \frac{\langle r_1 r_2 \rangle}{\sqrt{\langle r_1^2 \rangle \langle r_2^2 \rangle}}. \tag{0.11}$$

This measure (known in statistics and signal processing as *cosine similarity*) is the bivariate extension of the *MAmp* (0.1) measure and like *MAmp* is not sensitive to phase synchronization at all. Second, applying the normalization described in the previous section, the (linear) coherence measure becomes the (non-linear) phase-locking measure: in (0.9) now $r_1 = r_2 = 1$ and the denominator in (0.10) now equals 1, thus the coherence formula (0.10) simplifies to

$$PCoh = \left| \left\langle e^{i(\varphi_1 - \varphi_2)} \right\rangle \right|, \tag{0.12}$$

which is the bivariate extension of the *PCon* (0.4) measure. Having now all vectors unit length, that is, constant amplitude, *PCoh* is affected by phase synchronization, but not at all by amplitude co-modulation (Lachaux et al., 1999; Mormann et al., 2000; Rosenblum et al., 1996; Tass et al., 1998). For this reason and following several authors, we will refer to this measure as *Phase Coherence* (*PCoh*) instead that as phase-locking value (Mormann et al., 2000; Peraaza et al., 2012; Stam et al., 2007). Like coherence, phase coherence is sensitive to the concentration of the relative phase regardless its mean. That is to say, for this measure to be high, the *relative phase* between the two vectors must be stable across realizations, *regardless* where the vectors point in space. Unbiased estimators for phase coherence, which should be applied when a few realizations are available (<50), have been provided by Aydore et al., (2013) and Kutil (2012). Note that in the frequency domain *Coh* (0.10), *Com* (0.11) and *PCoh* (0.12) are defined in the

same way, with the only difference that the input complex numbers in this case are the output of the DFT.

In the same way we have done with the *PCon* measure, we may want to weight phase coherence using behavioral or experimental variables. For example, if w_k are the reaction times observed at *K* ERP sweeps, the *weighted phase coherence* shall be defined as

$$wPCoh = \frac{\left| \left\langle w e^{i(\varphi_{n1} - \varphi_{n2})} \right\rangle \right|}{\langle w \rangle} \ . \tag{0.13}$$

By evaluating the exponential at the phase frequency of another time-series (e.g., another source component or another scalp derivation), the *interareal phase-amplitude coupling (iPAC)* measure allows to assess the modulation of the time series 1 at the chosen amplitude frequency f_a by the phase frequency f_p of time-series 2, yielding

$$iPAC = \frac{\left| \left\langle r_{1f_a} e^{i\varphi_{2f_p}} \right\rangle \right|}{\left\langle r_{1f_a} \right\rangle} . \tag{0.14}$$

This measure is the bivariate extension of the PAC measure (0.7) and its interpretation is even more problematic. It allows to study how low-frequency waves (sometimes referred to as "carrier" waves) modulate high frequency oscillations in other regions and is useful when trying to model brain mechanisms related to large-scale synchronizations of neural assemblies (Llinas, 1988; Freeman, 2015; Palva and Palva, 2012; Varela et al., 2001).

Instantaneous and Lagged Phase Synchronization

A major limitation of measuring phase synchronization from two scalp signals is the spurious dependency resulting from the volume conduction and the arbitrariness of the measures with respect to the electrical reference (Lachaux et al., 1999; Lehmann et al., 2006; Nunez et al., 1997; Peraza et al., 2012; Srinivasan et al, 2007; Stam et al., 2007; Vinck et al., 2011; Winter et al., 2007). Since dipolar current generated in the brain diffuses instantaneously on the scalp even at large distances, two independent dipolar sources appear more dependent when measured at the scalp, especially if they are referenced to a common electrode (e.g., Peraza et al., 2012). To mitigate these effects it has been suggested to apply a Laplacian reference (Nunez et al., 1997; Winter et al., 2007) or to estimate dependency between voxels using a reference-

free source localization method (Lehmann et al., 2006). These attempts mitigates, but do not solve the problem. More effectively, it has been suggested to discard the *instantaneous* part of dependency to focus only on the *lagged* part; the cross-spectrum in (0.9) can be written in Cartesian coordinates as

$$c_{12} = z_1 z_2^* = \Re\left(c_{12}\right) + i\Im\left(c_{12}\right). \tag{0.15}$$

The real part of the cross-spectrum, named the *co-spectrum*, describes the *instantaneous synchronization*, that is, in-phase synchronization or out-of-phase synchronization. The imaginary part, named the *quadrature spectrum*, describes the synchronization with a quarter of a cycle lead or lag (Bloomfield, 2000). This is illustrated in Fig. 7.
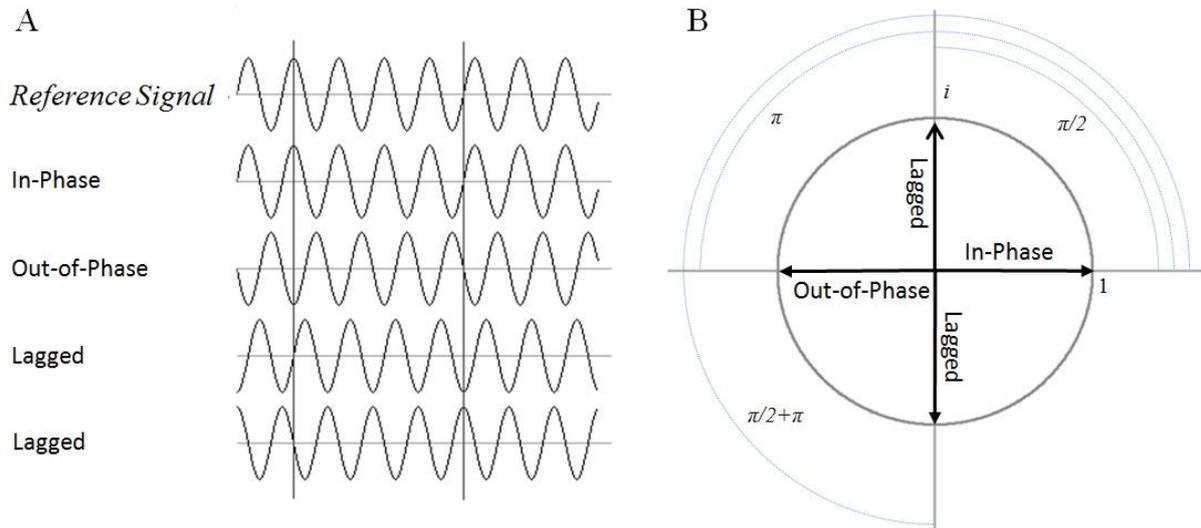

Figure 7: A) All sinusoidal waves have the same frequency and unitary amplitude, but different phase. With respect to the reference signal, the relative phase is 0 for the in-phase signal, π for the out-of-phase signal, $\pi/2$ and $\pi/2+\pi$ for the two lagged signals. Consider the modulus of the cross-spectrum c_{12} in (0.15) between the reference signal (first trace) and the other traces taken one at a time, given by the square root of $\Re^2\left(c_{12}\right) + \Im^2\left(c_{12}\right)$. It is equal to one for all the traces. In B) the contribution of the modulus for each trace is shown separately for the real part (co-spectrum) and imaginary part (quadrature spectrum). The square of the co-spectrum is one for the in-phase and out-of-phase signals and 0 for the two lagged signals. At the opposite, the quadrature spectrum is zero for the in-phase and out-of-phase signals and one for the lagged signal. Notice that considering the modulus of the cross-spectrum we cannot distinguish an in-phase from an out-of-phase relationship, that is why coherence (0.10) is analogous to the absolute value of correlation and not to correlation. Notice also that we cannot distinguish between the two lagged signals, that is why coherence does not provide information on which signal is leading and which one is lagging.

Since volume conduction is instantaneous, it may influence only the co-spectrum. Hence, several authors have proposed lagged coherence-like measures based on the quadrature spectra (Nolte et al., 2004, 2006; Pascual-Marqui, 2007; Stam et al., 2007; Vinck et al., 2011).

Nolte et al. (2004) defined the *imaginary coherence* (*ICoh*) as the coherence (0.10) where only the imaginary part of the cross-spectrum is retained, i.e.,

$$ICoh = \frac{\left|\left\langle \Im\left(c_{12}\right)\right\rangle\right|}{\sqrt{\left\langle c_1 \right\rangle \left\langle c_2 \right\rangle}} . \tag{0.16}$$

This measure has proven unsatisfactory with real data (Stam et al., 2007) and still makes use of the real part in the denominator of the formula. Pascual-Marqui (2007, Eq. 28) defined the *lagged coherence* (*LCoh*) measure applying to (0.16) a correction term in the denominator, as

$$LCoh = \frac{\left|\left\langle \Im\left(c_{12}\right)\right\rangle\right|}{\sqrt{\left\langle c_1 \right\rangle \left\langle c_2 \right\rangle - \left|\left\langle \Re\left(c_{12}\right)\right\rangle\right|}} . \tag{0.17}$$

The author also defined the instantaneous part of the coherence (in which only the co-spectrum is used), normalized versions of both lagged and instantaneous coherence (i.e., instantaneous and lagged *PCoh*) and multivariate versions of all these measures (Pascual-Marqui, 2007).

Stam et al. (2007) took a different path. They proposed the *phase-lag index* (*PLI*), which estimate the *asymmetry of the distribution of the relative phase*. It is given by

$$PLI = \left|\left\langle sign \, \Im\left(c_{12}\right)\right\rangle\right|, \tag{0.18}$$

where the *sign* function returns 1 if the relative phase vector is in the upper quadrants or -1 if it is in the lower quadrants. A weighted version of this measure, named *weighted phase-lag index* (*wPLI*), has been proposed by Vinck et al. (2011). It is given by

$$wPLI = \frac{\left|\left\langle \left|\Im\left(c_{12}\right)\right| sign \, \Im\left(c_{12}\right)\right\rangle\right|}{\left\langle \left|\Im\left(c_{12}\right)\right|\right\rangle} = \frac{\left|\left\langle \Im\left(c_{12}\right)\right\rangle\right|}{\left\langle \left|\Im\left(c_{12}\right)\right|\right\rangle} . \tag{0.19}$$

The rationale behind the *PLI* and *wPLI* measures is illustrated in Fig. 8.
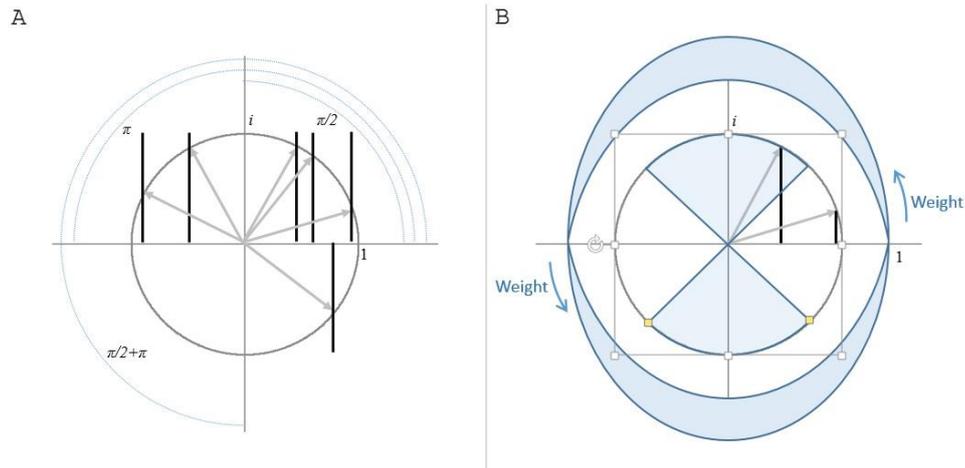
Figure 8: The left diagram is similar to those in Fig. 5 and 6, but now each grey vector represents normalized cross-spectra (0.15), i.e., relative-phase vectors. A) The phase-lag index (*PLI*) (0.18) considers the asymmetry of the distribution observed on the signs of the imaginary part of the cross-spectrum (y-axis), represented by black vertical lines of unitary length. In B) the imaginary part of two normalized cross-spectra is shown as a black vertical line. The white sectors of the circle delimitate the relative phase range in which the relative phase vectors are closer to 0 or π as compared to $\pi/2$ or $\pi/2+\pi$, i.e., they are closer to the real axis than to the imaginary axis. The white sectors indicate an *instantaneous* phase relationship between the two time-series, whereas the darkened sectors indicate a *lagged* phase relationship. The PLI is small if the relative phase vectors are uniformly distributed around the circle, like coherence and phase coherence. However, unlike these measures, PLI is small also if the relative phase vectors are centered around 0 and π, that is, if the phase relationship is instantaneous. The *wPLI* (0.19) acts similarly to the *PLI*, but in addition it weights the sign function proportionally to the distance of the relative phase from 0 or π (rearranged from Vinck et al. 2011).

Like the i*PAC*, the *PLI* and *wPLI* measures are currently used in studies that attempt to identify brain networks, for instance, by means of graph theory (Aydore et al., 2013; Palva and Palva, 2012; Peraza et al., 2012). Vinck et al. (2011) proposed an unbiased *PLI* and *wPLI* estimator that should be preferred when the number of realizations is low (<50). In a high-density EEG studies Hardmeier et al. (2014) found the *PLI* to have less global inter-subject variability and test-retest reliability as compared to the *wPLI*. In an oddball ERP study performed in noisy conditions (walking subjects) Lau et al. (2012) found the variance of the *wPLI* be very high. However the coefficient of variation[5] of the *wPLI* estimated on 500ms sliding windows featured very much lower variance. Furthermore, it reliably decreased on the average of all pair-wise electrodes in between 300 ms and 1s post-stimulus. It appears then that the variance of this estimator candidates as a useful index of phase synchronization more than the index itself.

---

[5] For a statistical sample the coefficient of variation is given by the standard deviation divided by the mean.

It should be kept in mind that all lagged measures here discussed are insensitive to instantaneous phase synchronization, thus are not adapted in general. For instance, if one is interested in brain coupling phenomena, that is, synchronization of EEG signal across individuals, the instantaneous phase synchronization cannot be explained by volume conduction and can therefore be analyzed.

Conclusions and Discussion

Special Considerations In Time-Frequency Domain Analysis.

Time-frequency and time-frequency dependency analysis requires special care. The Hilbert transform is obtained by the FFT algorithm (Marple, 1999). The FFT of a single realization provides an inconsistent estimates, in the sense that the variance of the estimator is proportional to the estimate itself and does not decrease with window size, thus some form of averaging and/or smoothing is always necessary (Thomson, 1982). In order to increase the consistency of the estimators, hence to minimize the number of points to be averaged, one can use multitaper FFT estimations (Thomson, 1982). The use of the FFT algorithm also requires the choice of a tapering window in the time domain to counteract spectral leakage due to finite window size (see Harris, 1978).

Regarding the Hilbert transform, the analytic signal does not necessarily represent adequately the phase of the original signal. The study of Chavez et al. (2006) has stressed that this is the case in general only if the original signal is a simple oscillator with a narrow-band frequency support. These authors have provided useful measures to check empirically the goodness of the analytic signal representation. Because of this limitation, for a signal displaying multiple spectral power peaks or broad-band behavior, which is the case in general of EEG and ERP, the application of a filter bank to extract narrow-band behavior is necessary. When applying the filter bank one should strive to enforce minimal distortion to the phase of the signal. In general, a finite impulse response filter with linear phase response is adopted (see Widmann et al., 2014, for a review). The choice of the filters band width and frequency resolution is usually a matter of trials and errors; the band width should be large enough to capture the oscillating behavior and small enough to avoid capturing several oscillators in adjacent frequencies. Also, the use of filter banks engenders edge effects, that is, severe distortions of the analytic signal at the left and right extremities of the time window under analysis (Mormann et al., 2000). This

latter problem is easily solved defining a larger time window centered at the window of interest and successively trimming an adequate number of samples at both sizes.

Regardless the chosen time-frequency representation, the estimation of phase and relative phase for realizations, time sample and frequencies featuring a low signal-to-noise ratio are meaningless; the phase being an angle, it is defined for vector of any length, even if the length (i.,e., the amplitude) is negligible. However, phase measures can be interpreted only where the amplitude is high (Bloomfield, 2000). The effect is exacerbated if we apply normalizations, since in this case very small coefficients are weighted as the others in the average, whereas they should better be ignored.

Those are just the most important aspects to be taken into consideration when dealing with frequency domain and time-frequency domain methods. A throughout discussion on these methods and their application can be found in Cohen (2014).

References

Aydore S, Pantazis D, Leahy RM. (2013) A note on the phase locking value and its properties. Neuroimage, 74, 231-44.

Bloomfield P. (2000) Fourier Anal ysis of Time Series. An Introduction (2nd Ed.). John Wiley & Sons, New York, 261 pp.

Burns A (2004) Fourier-, Hilbert- and wavelet-based signal analysis: are they really independent approaches? Journal of Neuroscience Methods, 137, 321-332.

Canolty RT, Edwards E, Dalal SS et al. (2006). High Gamma Power Is Phase-Locked to Theta Oscillations in Human Neocortex. Science, 313(5793), 1626–1628.

Chavez M., Besserve M., Adam C., Martinerie J. (2006) Towards a proper estimation of phase synchronization from time series. J Neurosci Methods. 154(1-2), 149-60.

Cohen M.X. (2014) Analyzing Neural Time Series Data. Theory and Practice, MIT Press, 600 pp.

Cohen MX, Cavanagh JF (2011) Single-trial regression elucidates the role of prefrontal theta oscillations in response conflict. Front. Psychol., 2, 30.

Colgin LL. (2015) Theta-gamma coupling in the entorhinal-hippocampal system. Curr Opin Neurobiol., 31, 45-50.

Congedo M, Gouy-Pailler C, Jutten C (2008) On the blind source separation of human electroencephalogram by approximate joint diagonalization of second order statistics. Clinical Neurophysiol, 119, 2677-2686.

Cooley J.W., Tukey J.W. (1965). An algorithm for the machine calculation of complex Fourier series. Math. Comput. 19, 297–301.

Freeman WJ. (2015) Mechanism and significance of global coherence in scalp EEG. Curr Opin Neurobiol., 31:199-205.

Frigo M., Johnson S.G. (2005) The design and implementation of FFTW3. Proceedings of the IEEE, 93(2), 216–231.

Gabor D. (1946) Theory of Communication. J IEE London, 93, 429-457.

Hardmeier M, Hatz F, Bousleiman H, Schindler C, Stam CJ, Fuhr P. (2014) Reproducibility of functional connectivity and graph measures based on the phase lag index (PLI) and weighted phase lag index (wPLI) derived from high resolution EEG. PLoS One. 9(10):e108648.

Harris F.J. (1978) On the use of windows for harmonic analysis with the discrete Fourier transform. Proceedings of the IEEE, 66, 51-83.

Kalitzin S., Parra J., Velis D.N., Lopes da Silva F.H. (2002) Enhancement of phase clustering in the EEG/MEG gamma frequency band anticipates transitions to paroxysmal epileptiform activity in epileptic patients with known visual sensitivity. IEEE Trans. Biomed. Eng. 49, 1279–1286.

Kutil R. (2012) Biased and Unbiased Estimation of the Circular mean resultant length and its variance. Statistics, 46(4), 549-561.

Lachaux J.-P., Rodriguez E., Martinerie J., Varela F.J. (1999) Measuring phase synchrony in brain signals. Hum Brain Mapp. 8(4), 194-208.

Lau TM, Gwin JT, McDowell KG, Ferris DP. (2012) Weighted phase lag index stability as an artifact resistant measure to detect cognitive EEG activity during locomotion. J Neuroeng Rehabil, 24, 9:47.

Lehmann D., Faber P.L., Gianotti L.R., Kochi K., Pascual-Marqui R.D. (2006) Coherence and phase locking in the scalp EEG and between LORETA model sources, and microstates as putative mechanisms of brain temporo-spatial functional organization. J Physiol Paris, 99(1), 29-36.

Le Van Quyen M., Foucher J., Lachaux J.-P., Rodriguez E., Lutz A., Martinerie J., Varela F.J. (2001) Comparison of Hilbert transform and wavelet methods for the analysis of neuronal synchrony. Journal of neuroscience methods, 111(2), 83-98.

Lisman, J. E. and O. Jensen (2013) The theta-gamma neural code. Neuron 77(6), 1002-1016.

Llinas, R. R. (1988). The intrinsic electrophysiological properties of mammalian neurons: insights into central nervous system function. Science 242(4886), 1654-1664.

Makeig S, Debener S, Onton J, Delorme A, (2004) Mining event-related brain dynamics. Trends in cognitive sciences 8 (5), 204-210.

Mardia K (1972) Statistics of Directional Data. Academic Press, New York.

Marple S.L. (1999) Computing the Discrete-Time Analytic Signal via FFT. IEEE Transactions on Signal Processing 47(9), 2600-3.

Marrelec G., Daunizeau J., Pélégrini-Issac M., Doyon J., Benali H., Conditional correlation as a measure of mediated interactivity in fMRI and MEG/EEG. IEEE Transactions on Signal Processing, 2005, 53(9):3503-3516.

Mormann F, Lehnertz K, David P, Elger CE. (2000) Mean phase coherence as a measure for phase synchronization and its application to the EEG of epilepsy patients. Physica D, 144, 358-369.

Nolte G., Bai O., Wheaton L., Mari Z., Vorbach S., Hallett M. (2004) Identifying true brain interaction from EEG data using the imaginary part of coherency. Clin Neurophysiol, 115(10), 2292-307.

Nolte G., Meinecke F.C., Ziehe A. Müller K.-R. (2006) Identifying interactions in mixed and noisy complex systems. Physical Review E, 73, #051913.

Nunez P.L., Srinivasan R., Westdorp A.F., Wijesinghe R.S., Tucker D.M., Silberstein R.B., Cadusch P.J. (1997) EEG coherency. I: Statistics, reference electrode, volume conduction, Laplacians, cortical imaging, and interpretation at multiple scales. Electroencephalogr Clin Neurophysiol. 103(5), 499-515.

Özkurt TE, Schnitzler A (2011) A crtitical note on the definition of phase-amplitude cross-frequency coupling. Journal of Neuroscience Methods, 201, 438-443.

Palva, S. and J. M. Palva (2012) Discovering oscillatory interaction networks with M/EEG: challenges and breakthroughs. Trends Cogn Sci 16(4): 219-230.

Pascual-Marqui R.D. (2007) Instantaneous and lagged measurements of linear and nonlinear dependence between groups of multivariate time series: frequency decomposition. arXiv:0711.1455

Peraza L.R., Asghar A.U.R, Green G., Halliday D.M. (2012) Volume conduction effects in brain network inference from electroencephalographic recordings using phase lag index. Journal of neuroscience methods, 207(2), 189-199.

Quain Quiroga R., Kraskov A., Kreuz T., Grassberger P. (2002) Performance of different synchronization measures in real data: A case study on electroencephalographic signals. Physical Review E, 65 (4), 041903.

Rosenblum M.G., Pikovsky A.S., Kurths J., (1996) Phase Synchronization of Chaotic Oscillators, Physical Review Letters, 76, 1804-1807.

Shaw J.C. (1981) An introduction to the coherence function and its use in EEG signal analysis. J Med Eng Technol., 5(6), 279-88.

Srinivasan R., Winter W.R., Ding J., Nunez P.L. (2007) EEG and MEG coherence: measures of functional connectivity at distinct spatial scales of neocortical dynamics. J Neurosci Methods, 166(1), 41-52.

Stam CJ, Nolte G, Daffertshofer A. (2007) Phase lag index: assessment of functional connectivity from multi channel EEG and MEG with diminished bias from common sources. Hum Brain Mapp, 28(11), 1178-93.

Tallon-Baudry C., Bertrand O., Delpuech C., Pernier J. (1996) Stimulus Specificity of Phase-Locked and Non-Phase-Locked 40 Hz Visual Responses in Human. Journal of Neuroscience, 16, 4240-4249.

Tass P., Rosenblum M.G. Weule J., Kurths J., Pikovsky A., Volkmann J., Schnitzler A., Freund H.-J., (1998) Detection of n:m Phase Locking from Noisy Data: Application to Magnetoencephalography. Phys. Rev. Lett. 81 (15), 3291-3294.

Thomson D.J. (1982) Spectrum estimation and harmonic analysis. Proceedings of the IEEE, 70, 1055–1096.

Varela, F., J. P. Lachaux, E. Rodriguez and J. Martinerie (2001). The brainweb: phase synchronization and large-scale integration. Nat Rev Neurosci 2(4), 229-239.

Vinck M., Oostenveld R., van Wingerden M., Battaglia F., Pennartz C. (2011) An improved index of phase synchronization for electrophysiological data in the presence of volume-conduction, noise and sample-size bias. NeuroImage, 55(4), 1548-1565.

Welch, P.D. (1967) The Use of Fast Fourier Transform for the Estimation of Power Spectra: A Method Based on Time Averaging Over Short, Modified Periodograms, IEEE Transactions on Audio Electroacoustics, AU-15, 70–73.

Widmann A., Schröger E., Maess B. (2014) Digital filter design for electrophysiological data - a practical approach. J Neurosci Methods. S0165-0270(14)00286-6.

Winter WR, Nunez PL, Ding J, Srinivasan R. (2007) Comparison of the effect of volume conduction on EEG coherence with the effect of field spread on MEG coherence. Stat Med., 26(21), 3946-57.